Geophysical imaging of the Paeroa Fault: Insights from a dense nodal seismic array

Brook Keats[1], Stephen Bannister[2], Cécile Massiot[2], Craig Miller[1], Stuart Henrys[2], Thomas Brakenrig[1], Lauren Coup[1], Nick Macdonald[1], Oujirou Kurimura[1], Lexus Werahiko[3], Usionae Werahiko-Mita[3], Michelle Phillips[3] and Chengxin Jiang[4]

[1] GNS Science, Wairakei Research Centre, Taupō

[2] GNS Science, Avalon, Lower Hutt

[3] Ngati Tahu – Ngati Whaoa

4 Australian National University, Canberra, Australia

b.keats@gns.cri.nz

Keywords: *Seismology, dense nodal seismic array, ambient noise, Paeroa fault.*

ABSTRACT

The Paeroa Fault is one of the longest and most active multi-strand faults in the Taupō Rift, capable of generating Mw6.8+ ruptures on a millennial timescale. At its northern end the Paeroa Fault splays into the Ngapouri fault and is surrounded by several active geothermal features. Mapping the fault strands and their dip angle is important to understand earthquake hazards, fluid flow pathways and links between faulting, volcanism, and geothermal activity.

Over the summer of 2023/24 we deployed a dense nodal seismic array (DNSA) across the northern termination of the Paeroa fault, straddling the deep resistivity boundary along the northern boundary of the Waiotapu and Waimangu geothermal systems. The survey deployed 147 short-period and broadband nodal seismometers recording continuously for a period of ~4 weeks and collected new closely spaced gravity data.

In the initial analysis we have cross-correlated and stacked more than 1000 station-station pairs. The derived dispersion spectra for station-station pairs show clean fundamental surface-wave dispersion for Z-Z components for frequencies between 0.3 and 2 Hz. We will apply additional processing approaches to also retrieve higher modes, and to retrieve information for a wider bandwidth. We will then jointly invert the Rayleigh and Love dispersion curves to construct a three-dimensional S-wave velocity model, likely imaging to c. 2 km in depth across the spatial extent of the array for combined interpretation with a new 3D gravity model of the area. We anticipate that our derived 3-D S-wave velocity model will reflect the subsurface heterogeneity across the Paeroa Fault, as well as imaging the northern boundary of the Waimangu and Waiotapu geothermal systems, delineating subsurface faults associated with local seismicity.

With this study we aim to show that DNSA surveys are an effective non-invasive geophysical method for imaging shallow faults in the TVZ, for seismic hazard planning and geothermal exploration.

1. INTRODUCTION

The Paeroa fault is one of the largest faults in the Taupō Volcanic Zone (TVZ), extending ~30 km from SW to NE and capable of generating Mw 6.8+ earthquakes on a millennial timescale (Berryman et al., 2008). It splays ENE into the Ngapouri fault on its northern end. Numerous strands are mapped on the surface, suggesting a complex subsurface structure of interconnected fault planes. It passes through the Waikite Geothermal Field and terminates in the north on the south-western margin of the Okataina Volcanic Centre (OVC), a few kilometers west of Waimangu Volcanic Valley. The Ngapouri fault splay to the west passes through the Waiotapu Geothermal Field (Figure 1). The northern end of the fault is therefore an ideal site for trialling passive seismic techniques in the TVZ, and investigating the link between faulting, volcanism, and geothermal activity.

1.1 Geological setting

The Paeroa fault is a normal fault located near the eastern margin of the Taupō Rift in the TVZ. This ~60 km wide structure extends north-east from Mount Ruapehu out to White Island offshore in the Bay of Plenty, with extension rates progressively increasing from ~5 to ~15 mm/yr northwards (Seebeck et al., 2014, Wilson & Rowland, 2016).

The Paeroa fault is one the largest structures in the Taupō Rift. It is downthrown to the west, and visible as a ~500 m high escarpment separating the Taupō – Reporoa basin from Waikite valley. Twenty-two rupture events have been recognized in the last ~16 ka, often associated with volcanism at the OVC to the north-east (Berryman et al., 2008). Links between volcanism and faulting is also evident on the Ngapouri fault (Berryman et al., 2022).

Direct current resistivity data from Bibby et al., 1995 shows a sharp transition from low to high apparent resistivity occuring between the Paeroa and Ngapouri faults, with resistivity increasing to the north-west (Figure 2). This transition was interpreted to be due to ~1 km offset across the Paeroa fault, with low resistivity shallow clays associated with local geothermal surface features to the east replaced by young (< 1 Ma) volcanics west of the fault (Risk et al., 1999).

1.2 Seismological hazard

The subsurface structure, dip magnitude, and interconnectivity, of the Paeroa fault and other large faults in the region (e.g. the Horohoro fault) are currently poorly

ISSN 2703-4275

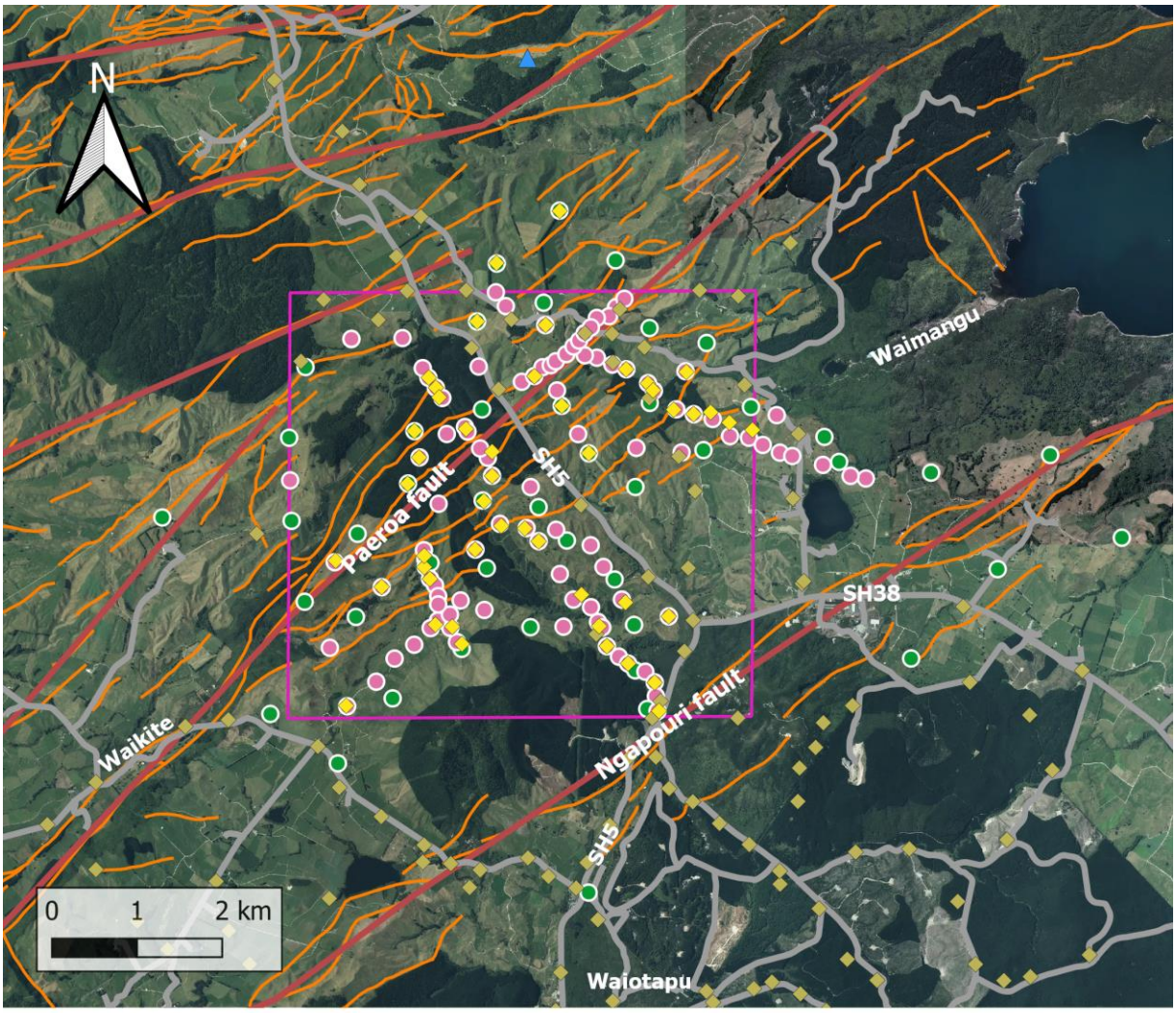

Legend

DNSA network
- Broadband nodes
- Short-period nodes

GeoNet
- GeoNet broadband stations
- GeoNet short-period stations

Gravity data
- Existing gravity data
- New gravity data

Faults
- NZ_CFM_v1_0
- NZAFD_Oct_2022

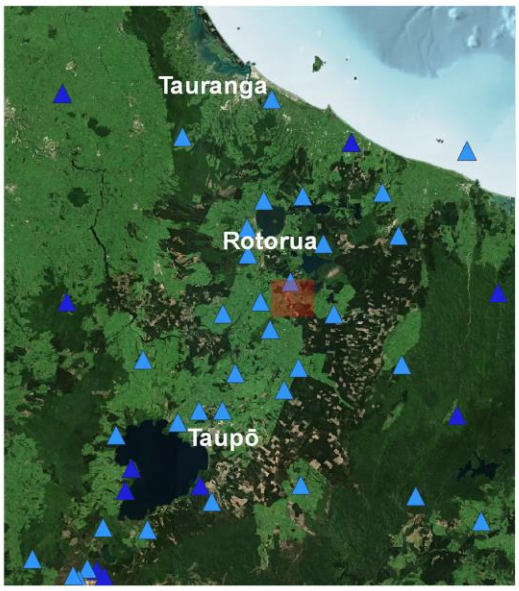

Figure 1: Paeroa fault study area, highlighted in red on the regional map. The primary area of investigation is highlighted by the purple rectangle in the primary map. Roads are marked as grey lines, with State Highway 5 and 38 labelled as SH5 and SH38. The geothermal areas of Waikite, Waiotapu and Waimangu are labelled. Red lines mark fault traces from the Community Fault Model (NZ_CFM_v1_0), and orange lines mark mapped faults from the NZ Active Fault Database (NZAFD_Oct_2022).

constrained. This results in uncertainty for estimating their seismic hazard potential. For example, in the Community Fault Model (CFM, Seebeck et al., 2023) the Paeroa fault is simplified to a single strand with a dip angle of 60°. This value is derived from standard fault models and shallow (~5 m deep) paleoseismic trenches. If its dip angle was instead closer 30°, its rupture area and maximum magnitude would increase by ~70%. The Edgecumbe fault to the north-east was estimated to have a dip of ~32° at depth (Webb and Anderson, 1998), while geothermal borehole data suggest dip angles of 70-90° are common at 2-3 km depth in the Taupō Rift (McNamara et al., 2019; Massiot et al., 2023). Resolving the uncertainty on the Paeroa Fault geometry would therefore improve the CFM, and the National Seismic Hazard Model (NSHM, Gerstenberger et al., 2023).

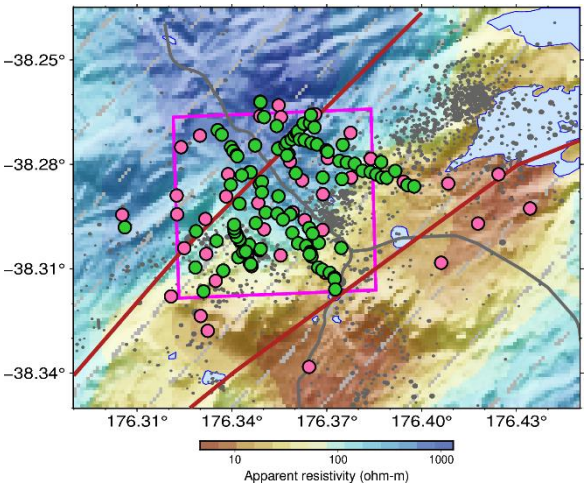

Figure 2: Apparent resistivity across the Paeroa and Ngapouri faults. Legend follows Figure 1. Resistivity data from Bibby et al., 1995. Grey circles show the locations of shallow seismicity events, from Bannister et al (2022).

2. DATA

2.1 Geophysical surveys

A geophysical survey, incorporating a Dense Nodal Seismic Array (DNSA), and new gravity measurements was carried out over the summer of 2023/24.

2.1.1 Seismic survey

The DNSA survey made use of a set of short-period and broadband nodal seismometers from the Australian National Research Facility for Earth Sounding (ANSIR). The short-period instruments were SmartSolo IGU-16HR 3C 5 Hz nodal seismometers, and the broadband instruments were SmartSolo IGU-BD3C-5 0.2 Hz nodal seismometers, configured to sample at 250 Hz. The seismometers were deployed over a roughly 10x10 km study area, with primarily broadband instruments deployed at coarse (0.5-1 km) spacing around the perimeter. Instrument spacing was progressively reduced towards the centre of the survey, with short-period instruments deployed at ~100 m spacing in linear arrays in areas of interest running parallel and perpendicular to the strike of the Paeroa fault. The 101 short-period and 45 broadband nodes were deployed from 4-12th of December 2023, and retrieved on 8-11th of January 2024, recording continuously to retrieve background ambient noise at 250 Hz for approximately 1 month.

2.1.2 Gravity survey

47 new gravity measurements were made using a Lacoste & Romberg G meter (G106) alongside the DNSA installation. Readings were made at gravity reference station ACNN, ~8 km south of Reporoa, at the start and end of each day to convert the data to absolute gravity values and record instrument drift. The survey used a looping method to obtain repeat measurements at survey sites throughout each survey day to more accurately record instrument drift and allow the new datapoints to be recorded with a high level (µgal) of precision. Measurement locations were recorded using post processed differential GNSS, obtaining vertical and horizontal accuracies of 0.1m equivalent to gravity accuracies of 0.03mGal.

3. METHODS

The seismic data were analysed using ambient noise cross correlation methods. The gravity data were processed to a complete Bouguer anomaly and incorporated into a regional dataset.

3.1 Seismic processing

Processing the seismic data was focused on deriving group and phase velocity dispersion information from the ambient seismic noise. The group and phase velocity measurements, derived for each possible pair of seismometers, can then be used to derive 3-D velocity images for the earth volume beneath the array. The continuous raw broadband and short-period data were first cut into 12-hour segments and down-sampled to a 20 Hz sample rate. These segments were then demeaned, detrended, normalised in the temporal domain, whitened in the frequency domain (Benson et al, 2007) and band-pass filtered. Cross-correlations were then estimated between all seismometer combinations, using 20-minute cross-correlation windows with 15-minute steps, using *Noisepy* software (Jiang and Denolle, 2020). The resulting cross-correlations were stacked, before dispersion analysis was carried out on the stacked cross-correlation for each seismometer pair.

3.2 Gravity processing

After drift and Earth tide removal, gravity data were processed to complete Bouguer anomaly (CBA) using a correction density of 2670kg/m^3. Terrain effects including that of bathymetry were calculated out to 167 km. A regional field representing the long wavelength effects of lower crustal and mantle density structure (Stagpoole et al., 2021) was removed from the CBA to obtain a residual anomaly map (Fig. 2) representing the upper crustal structure.

4. RESULTS

4.1 DNSA results

Stacking Z-Z cross correlation results between 0.5 – 10 s periods (0.1 – 2 Hz) against station distance reveals coherent symmetric peak of energy out to 6 km at ~2.8 s delay time for both positive (causal) and negative (acausal) values (Figure 3). Using the rule of thumb that Rayleigh phase velocities are most sensitive to shear-wave velocity structure at around 1/3 of their wavelength, this gives an average S-wave phase velocity of ~2.15 km/s across the study area down to ~2 km depth.

Group velocity analysis shows good dispersion information is retrieved for most seismometer pairs between 1 and 5 second period (0.2-to-1 Hz). Figure 3 shows an image of the group velocity versus the period (in seconds) for a single seismometer pair, derived using the stacked symmetric part of the cross-correlation function (CCF). The picked dispersion curve follows well-defined ridges in the velocity-period image (Figure 3) but is limited to periods below c. 4-5 seconds by seismic wavelength considerations. This single dispersion curve could be inverted (e.g. using Monte Carlo approaches) for a 1-D velocity-vs-depth function, but our intent is to carry out a full 3-D inversion using c.1000 such dispersion curves.

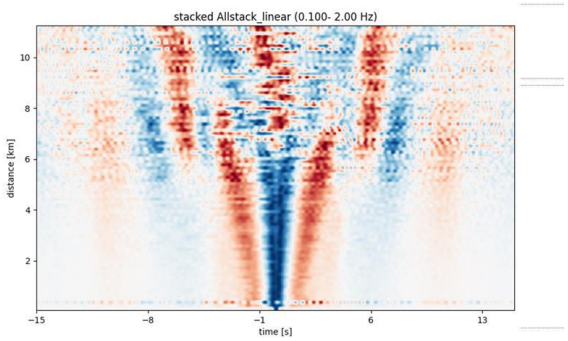

Figure 3: Moveout image from ZZ cross correlations in the 0.1 – 2 Hz frequency range (0.5 – 10 s period). A consistent single energy peak is present out to 6 km, giving a moveout velocity of ~2.15 km/s.

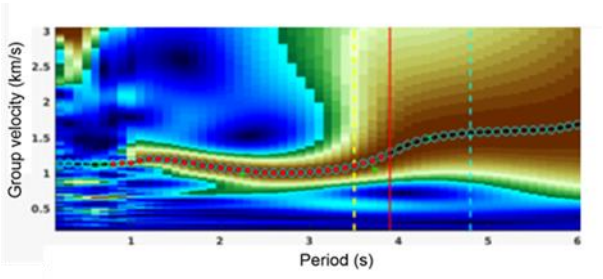

Figure 4: Image of group velocity (km/s) vs period (s) for a single pair of seismometers 7.4 km apart. The red dots show the picked dispersion curve for this station pair. This group velocity dispersion curve is then used as a guiding reference for subsequent phase velocity dispersion analysis.

4.2 Gravity results

The gravity data were integrated into the GNS gravity database, including data from Okataina Volcanic Center to the north (Miller et al. 2022). The survey significantly improved the density of gravity measurements across the Paeroa fault, particularly west of SH5. The new data refine the gravity gradients associated with the Paeroa fault and show additional complexity where the gravity trend rotates to the north. Later forward modelling with be undertaken to define the vertical offset across the fault.

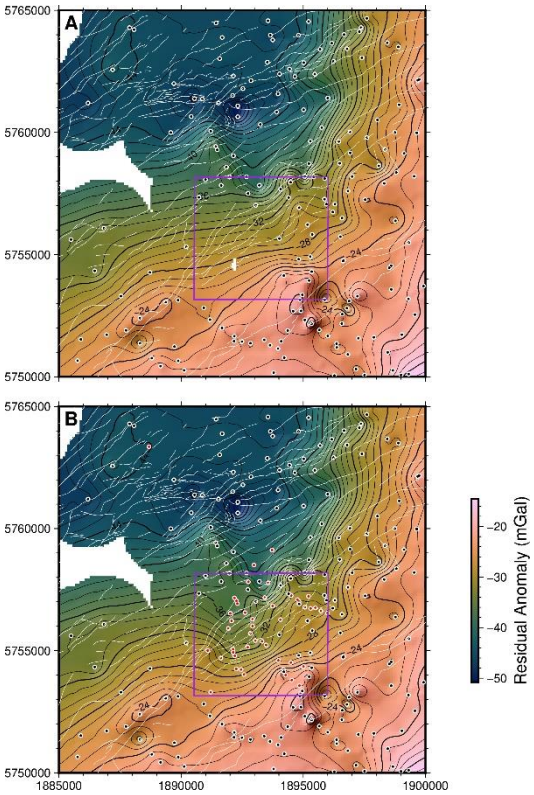

Figure 5: Residual gravity anomaly map showing a) the anomaly from the data points in the national gravity data base (black circles), and b) with the newly acquired datapoints (red circles) incorporated.

5. DISCUSSION

Active source seismic studies have a poor record in the TVZ, with high attenuation associated with poorly consolidated volcanics proving to be a limiting factor in previous surveys (Henrys and Hochstein, 1990, Lamarche, 1992). Earthquake tomography studies have successfully resolved large scale structures (Stern et al., 2010, Bannister et al., 2022), but lack the resolution necessary to characterise near surface fault structures. Electromagnetic methods (resistivity, magnetotellurics, e.g., Bibby et al., 1995, Bertrand et al., 2015) have proven to be adept at delineating the boundaries and extent of geothermal fields, but the physical properties of the earth that they sample often do not vary across fault planes, so they can also struggle to image fault structures.

With the arrival of nodal seismometers in the past decade, large scale seismic networks (e.g., DNSA's) can now be deployed quickly and efficiently over wide areas. Combining advances in computing power and digital data processing methods over the last few decades with DNSA's may allow passive seismic methods to overcome the limitations of earlier active seismic surveys and prove themselves as an effective tool for characterising the shallow subsurface in highly attenuative places like the TVZ. This could provide a new way for imaging the dip angle, and interconnectivity, of large faults like the Paeroa fault. This would improve fault parameters in the CFM and the NSHM, leading to improved risk modelling in the region, and a better understanding of their hazard. They may also find applications in the geothermal sector, to improve targeting of faults during the

exploration of new fields, or to better characterise existing resources.

6. CONCLUSIONS

We have shown that ambient noise analysis, combined with DNSA's, can successfully retrieve S-wave velocity structure from the shallow subsurface in the TVZ. While our analysis is at an early stage, the results presented here indicate that we will be able to use these techniques to invert this dataset for 3-D S-wave velocity structure across the Paeroa fault.

Combining this with the updated residual gravity anomaly obtained during this survey will lead to a more accurate 3-D model of the fault strands and provide a reliable constraint on its dip magnitude angle.

ACKNOWLEDGEMENTS

We would like to thank Michelle Phillips of Ngati Tahu – Ngati Whaoa Runanga Trust for partnering with us on this project and arranging for two local rangatahi to work with us as field assistants during the survey. Ngati Tahu – Ngati Whaoa are mana whenua for the area where the Paeroa fault predominantly sits. We also thank local landowners for providing us access to their properties during the survey.

This project is supported by a Natural Hazards Commission Toka Tū Ake (formerly the Earthquake Commission) biennial grant, and a GNS Science Capability Development Fund grant.

Nodal seismometers for this project were provided by the AuScope National Research Facility for Earth Imaging (ANSIR), based at the Australia National University (ANU).

Ambient seismic noise processing was carried out using the *noisepy* software package (Jiang and Denolle, 2020). Thanks to Huajian Yao for use of his EGFAnalysis dispersion software.

REFERENCES

Bannister, S., Bertrand, E.A. Heimann, S. Bourguignon, S., Asher, C., Shanks, J., Harvison, A., 2022. Imaging sub-caldera structure with local seismicity, Okataina Volcanic Centre, Taupo Volcanic Zone, using double-difference seismic tomography. *J.Volcanology and Geothermal research*, v431, 107653.

Benson, G.D., Ritzwoller, M.H., Barmin, M.P., Levshin, A.L., Lin, F., Moschetti, M.P., Shapiro, N.M., and Yang, Y (2007). Processing seismic ambient noise data to obtain reliable broad-band surface wave dispersion measurements. *Geophys.J.Int*, v169, 1239-1260.

Berryman, K., Villamor, P., Nairn, I., van Dissen, R., Begg, J., & Lee, J. (2008). Late pleistocene surface rupture history of the paeroa fault, Taupo Rift, New Zealand. *New Zealand Journal of Geology and Geophysics*, *51*(2), 135–158. https://doi.org/10.1080/00288300809509855

Berryman, K., Villamor, P., Nairn, I., Begg, J., Alloway, B. v., Rowland, J., Lee, J., & Capote, R. (2022). Volcano-tectonic interactions at the southern margin of the Okataina Volcanic Centre, Taupō Volcanic Zone, New Zealand. *Journal of Volcanology and Geothermal Research*, *427*. https://doi.org/10.1016/j.jvolgeores.2022.107552

Bertrand, E. A., Caldwell, T. G., Bannister, S., Soengkono, S., Bennie, S. L., Hill, G. J., & Heise, W. (2015). Using array MT data to image the crustal resistivity structure of the southeastern Taupo Volcanic Zone, New Zealand. *Journal of Volcanology and Geothermal Research*, *305*, 63–75. https://doi.org/10.1016/j.jvolgeores.2015.09.020

Bibby, H. M., Caldwell, T. G., Davey, F. J., & Webb, T. H. (1995). Geophysical evidence on the structure of the Taupo Volcanic Zone and its hydrothermal circulation. In *Journal of Volcanology and Geothermal Research* (Vol. 68).

Gerstenberger, M. C., Stirling, M. W., Mcverry, G., & Rhoades, D. A. (n.d.). *The New Zealand National Seismic Hazard Model: Rethinking PSHA*.

Henrys, S. A., & Hochstein, M. P. (1990). GEOPHYSICAL STRUCTURE OF THE BROADLANDS-OHAAKI GEOTHERMAL FIELD (NEW ZEALAND). *Geothermics*, *19*(2), 129–150.

Jiang, C., and Denolle, M. (2020). NoisePy: a new high-performance python tool for seismic ambient noise seismology. *Seismological Research Letters* 91, no. 3, 1853-1866.

Lamarche, G. (1992). *SEISMIC REFLECTION SURVEY IN THE GEOTHERMAL FIELD OF THE ROTORUA CAIJDERA, NEW ZEALAND* (Vol. 21, Issue 1).

Massiot, C., Milicich, S. D., Sepulveda, F., Sophy, M. J., Lawrence, M. J. F., Griffin, A. G., Rickman, M., Carson, L. B., Rosenberg, M., Simpson, M., Science, G. N. S., Hutt, L., Zealand, N., & Energy, C. (2023). Highlights of Borehole Imaging, Tauhara Geothermal Field Drilling, New Zealand. Proceeding World Geothermal Congress, Beijing, China, April 17-21, 2023.

McNamara, D. D., Milicich, S. D., Massiot, C., Villamor, P., Mclean, K., Sépulveda, F., & Ries, W. F. (2019). Tectonic controls on Taupo Volcanic Zone geothermal expression: Insights from Te Mihi, Wairakei Geothermal Field. Tectonics, 38, 3011–3033. https://doi.org/10.1029/2018TC005296

Miller, C. A., Barretto, J., Stagpoole, V., Caratori-Tontini, F., Brakenrig, T., & Bertrand, E. (2022). The integrated history of repeated caldera formation and infill at the Okataina Volcanic Centre: Insights from 3D gravity and magnetic models. *Journal of Volcanology and Geothermal Research*, *427*, 107555. https://doi.org/10.1016/j.jvolgeores.2022.107555

Seebeck, H., Dissen, R.V., Litchfield, N., Barnes, P.M., Nicol, A., Langridge, R., Barrell, D.J., Villamor, P., Ellis, S., Rattenbury, M. and Bannister, S., 2023. The New Zealand Community Fault Model–version 1.0: an improved geological foundation for seismic hazard modelling. *New Zealand Journal of Geology and Geophysics*, pp.1-21.

Seebeck, H., Nicol, A., Villamor, P., Ristau, J., & Pettinga, J. (2014). Structure and kinematics of the Taupo Rift, New Zealand. *Tectonics*, *33*(6), 1178–1199. https://doi.org/10.1002/2014TC003569

Stagpoole, V., Miller, C., Caratori Tontini, F., Brakenrig, T., & Macdonald, N. (2021). A two million-year history of rifting and caldera volcanism imprinted in new gravity anomaly compilation of the Taupō Volcanic Zone, New Zealand. *New Zealand Journal of Geology and Geophysics*, *64*(2–3), 358–371. https://doi.org/10.1080/00288306.2020.1848882

Stern, T., Stratford, W., Seward, A., Henderson, M., Savage, M., Smith, E., Benson, A., Greve, S., & Salmon, M. (2010). Crust-mantle structure of the central North Island, New Zealand, based on seismological observations. *Journal of Volcanology and Geothermal Research*, *190*(1–2), 58–74. https://doi.org/10.1016/j.jvolgeores.2009.11.017

Webb, T. H., & Anderson, H. (1998). Focal mechanisms of large earthquakes in the North Island of New Zealand: slip partitioning at an oblique active margin. *Geophys. J. Int*, *134*, 40–86. https://academic.oup.com/gji/article/134/1/40/632613

Wilson, C. J. N., & Rowland, J. v. (2016). The volcanic, magmatic and tectonic setting of the Taupo Volcanic Zone, New Zealand, reviewed from a geothermal perspective. *Geothermics*, *59*, 168–187. https://doi.org/10.1016/j.geothermics.2015.06.013